RAPID COMMUNICATIONS

PHYSICAL REVIEW B VOLUME 43, NUMBER 8 15 MARCH 1991-I

Surface phonons and structure of epitaxial nickel layers on Cu(001)

Y. Chen and S. Y. Tong
Department of Physics and Laboratory for Surface Studies, University of Wisconsin-Milwaukee, Milwaukee, Wisconsin 53201

Jae-Sung Kim, M. H. Mohamed,* and L. L. Kesmodel
Department of Physics, Indiana University, Bloomington, Indiana 47405
(Received 19 November 1990)

We compare measured and calculated electron-energy-loss phonon spectra of ultrathin films of Ni grown on Cu(001) to determine the interlayer spacings of the Ni layers. We find a small (~4.6%) expansion in the surface volume of the Ni film at two and four monolayers. Data of Ni-film modes along the $\bar{\Gamma}\bar{M}$ and $\bar{\Gamma}\bar{X}$ directions are measured for different thicknesses of the Ni film, and comparison between measured and calculated phonon dispersions of the film modes show considerable relaxation in the intralayer force constant of the overlayer film.

With modern deposition techniques, an increasing number of materials can be grown epitaxially on single-crystal substrates. Such ultrathin films, grown pseudomorphically with the underlying substrate, are found to exhibit striking magnetic, chemical, or optical properties.[1-10] There is also a great deal of interest in understanding the structure of these ultrathin films. However, to date, the structure of only a few ultrathin overlayer films has been quantitatively determined.[2,8-10] In this paper, we present experimental data and a theoretical analysis of vibrational modes specific to the ultrathin film, for two and four monolayers (ML) of nickel on Cu(001). These film modes have vibrational amplitudes confined primarily in the Ni overlayers. By studying their inelastic electron-energy-loss cross section as a function of scattering geometry, detailed layer-by-layer structural information (e.g., $\Delta d_\perp \leq \pm 0.1$ Å) is obtained for the overlayer film. We have also studied the dispersion relation of the film modes and find that there is a significant lowering in the frequency of these modes. This suggests considerable softening in the interlayer and intralayer force constants in the Ni film. The study also explains why Ni-film modes have been resolved experimentally by high-resolution electron-energy-loss spectroscopy (HREELS) along the $\bar{\Gamma}\bar{X}$ direction but not along the $\bar{\Gamma}\bar{M}$ direction.

All the experiments are performed in an ultrahigh-vacuum chamber with a base pressure in the low-10^{-11}-Torr range. The Cu(001) substrate is cleaned and characterized as described previously.[11] Ni films are prepared by evaporation of Ni onto the Cu substrate near room temperature and subsequent annealing up to 500 K. We find no interdiffusion of Ni and Cu as judged from a comparison of Auger-electron-spectroscopy (AES) spectra taken before and after annealing. The sharp $p(1\times1)$ low-energy electron-diffraction (LEED) patterns of these films show the pseudomorphic growth of Ni films on the Cu(001) substrate surface.

The thickness of the Ni film is monitored by means of a quartz-crystal oscillator and calibration of AES spectra. Surface-phonon spectra are measured at room temperature by HREELS. The spectrometer consists of a double-pass monochromator and single-pass analyzer as described earlier. The resolution is set to 40–60 cm^{-1} full width at half maximum. We employ various primary electron energies tuned for the highest scattering cross sections of the different phonon modes.

General vibrational properties of epitaxial films of Ni on Cu(001) have been studied by theoretical models.[12] The earlier calculations predicted the existence of localized film modes, whose frequencies lie above the Cu bulk band. The number of these film modes and their frequencies increase as the film's thickness is increased. In Fig. 1, we show the calculated dispersion for the case of 4-ML Ni on Cu(001). The calculation uses a nearest-neighbor central-force model with bulk force constants for the Ni and Cu layers, and an averaged $k_{\text{Ni-Cu}}=(k_{\text{Cu}}+k_{\text{Ni}})/2$ force constant for the Ni-Cu interface. A slab of 61 layers is used. From Fig. 1, besides the gap modes, the shear horizontal mode S_1 (at $\bar{X}$), and the Rayleigh modes S_4 (at $\bar{X}$) and S_1 (at $\bar{M}$), we identify four-film modes along $\bar{\Gamma}\bar{X}$ and six along $\bar{\Gamma}\bar{M}$ above the Cu bulk band. The polariza-

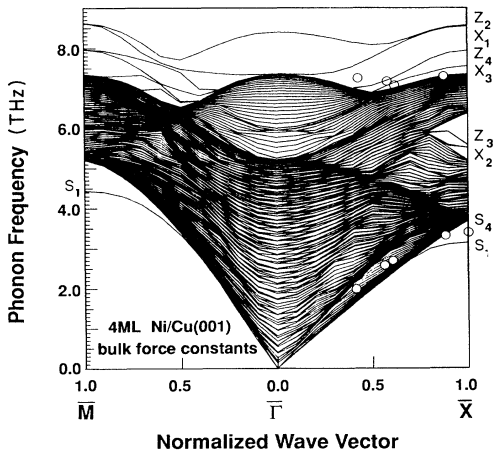

FIG. 1. Calculated phonon-dispersion curves along high symmetry directions $\bar{M}$-$\bar{\Gamma}$-$\bar{X}$ for 4-ML Ni/Cu(001) using a nearest-neighbor bulk central-force-constant model. The data are shown as open circles.

TABLE I. Force constants (10^{13} dyn/cm) used in the lattice-dynamical calculations for 4-ML Ni/Cu(001) and 2-ML Ni/Cu(001) (a is the nearest-neighbor distance)

		Force constants (10^{13} dyn/cm)	Ratio with k_{Ni} (bulk)
Ni-Ni (interlayer)	ϕ''	30.32	0.8
Ni-Ni (intralayer)	ϕ''	18.95	0.5
Ni-Ni (intralayer)	ϕ'/a	4.5	. . .
Ni-Cu	ϕ''	28.138	. . .
Cu-Cu	ϕ''	28.138	$=k_{Cu}$ (bulk)

tion at $\bar{X}$ and the thickness dependence of these modes are indicated in the figure. In this convention, $\hat{\mathbf{z}}_i, \hat{\mathbf{x}}_i, \hat{\mathbf{y}}_i$ indicate, respectively, shear vertical, longitudinal, and horizontal polarizations of the first-layer displacement of the film mode. The index i indicates the overlayer thickness at which the film mode first appears above the Cu bulk band based on this force-constant model.

Measured phonon dispersions along the $\bar{\Gamma}\bar{M}$ (Ref. 13) and $\bar{\Gamma}\bar{X}$ (Ref. 14) directions have been reported previously. In this paper, we present additional data along $\bar{\Gamma}\bar{X}$ and $\bar{\Gamma}\bar{M}$. The measured film modes appear as a separate peak (from that of the Rayleigh S_4 mode) along $\bar{\Gamma}\bar{X}$. We show the data as open circles in Fig. 1. There is clear disagreement between the data and the calculated phonon dispersion based on bulk force constants. For example, the measured frequencies lie ~ 30 cm^{-1} below those of the calculated Z_2 and X_1 modes for 4-ML Ni/Cu(001). This suggests considerable softening of the force constants in the film. To fit the data, we reduce the Ni-film interlayer force constant by 20% and the intralayer force constant by 50%. A positive first derivative of the pairwise potential is also included for each Ni layer. The modified force constants in the Ni film are listed in Table I. The calculated dispersion curves using the modified force constants are shown in Fig. 2. There is now very good agreement between theory and data (again shown as open circles). Besides lowering the Z_2 and X_1 film modes along $\bar{\Gamma}\bar{X}$, the Rayleigh mode S_4 appears inside the Cu band at most wave vectors, in good agreement with the data.

The lattice-dynamical calculations generate atomic displacements for all the modes of the 4-ML Ni/Cu(001) system. Using these as inputs, we calculate the electron-energy-loss spectra for different scattering geometries corresponding to different wave vectors in the two-dimensional Brillouin zone. The loss spectra have been shown to be very sensitive to the surface structure.[15,16]

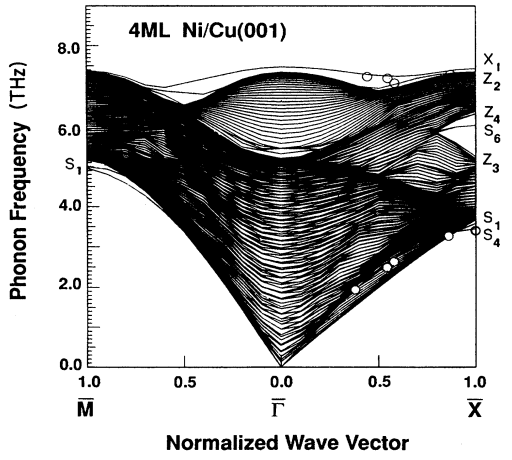

FIG. 2. Same as in Fig. 1, but the modified force constants listed in Table I are used and the optimal Ni-layer relaxation is included in the dispersion calculation. The same data as in Fig. 1 are shown as open circles.

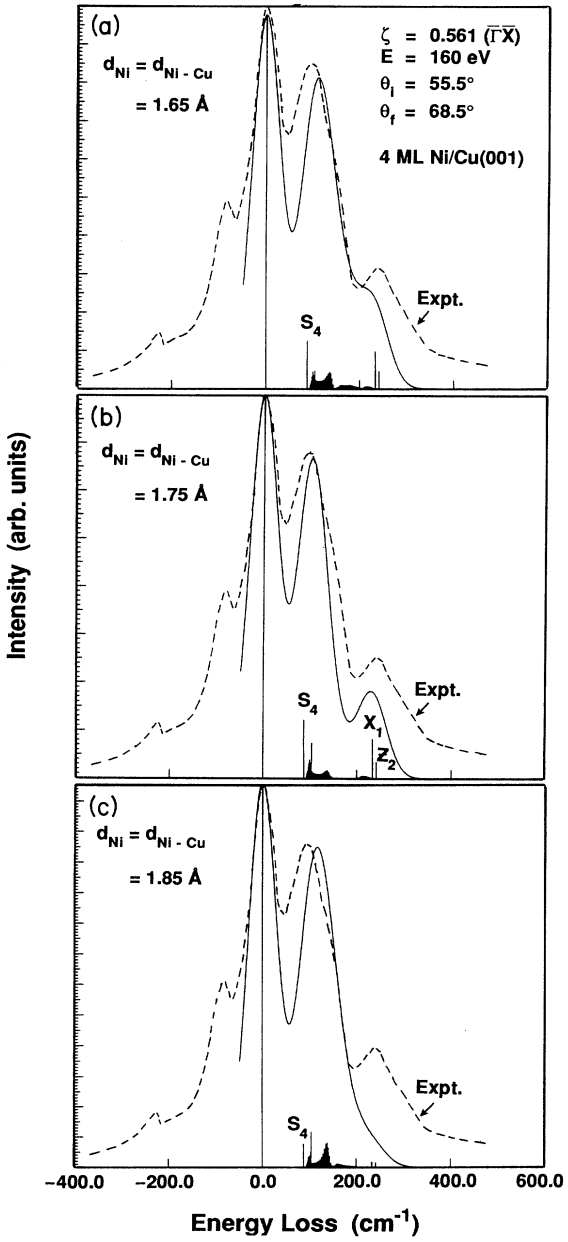

FIG. 3. Calculated (solid line) and measured (dashed line) electron-energy-loss cross-section spectra along the $\bar{\Gamma}\bar{X}$ direction. The values of the distance between Ni layers (d_{Ni}) in the film and between Ni-Cu layers are shown.

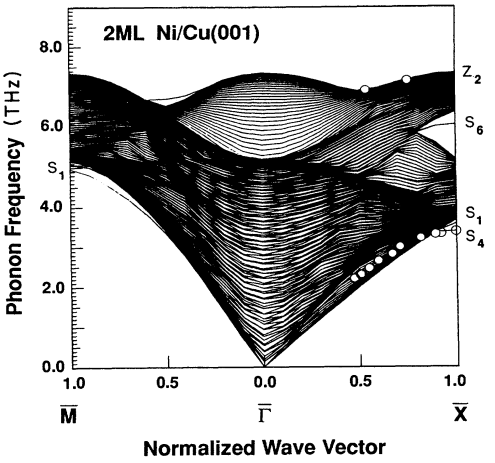

FIG. 4. Same as in Fig. 2, but for 2-ML Ni/Cu(001). The data for this system are shown as open circles.

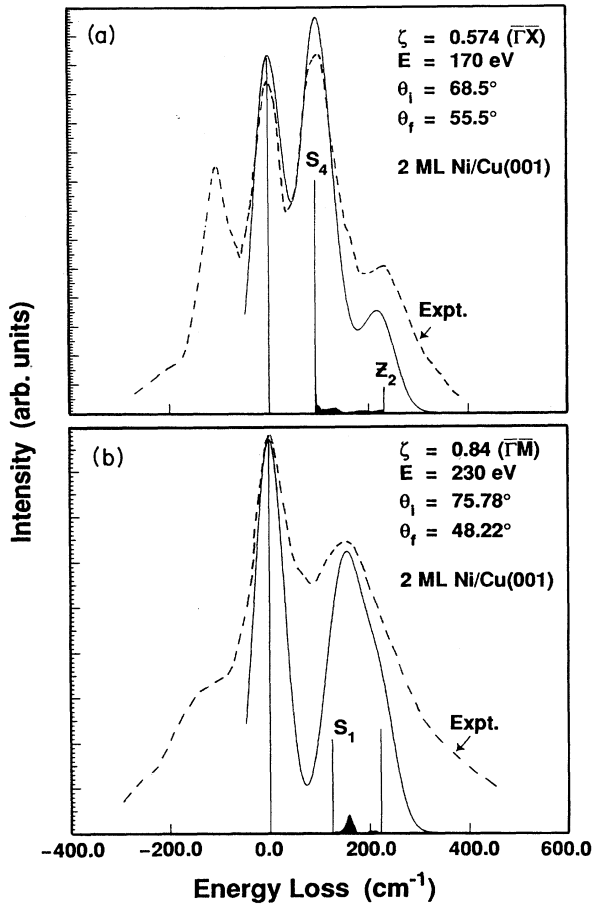

FIG. 5. Calculated (solid line) and measured (dashed line) electron-energy-loss cross-section spectra along (a) $\bar{\Gamma}\bar{X}$ and (b) $\bar{\Gamma}\bar{M}$ directions for 2-ML Ni/Cu(001) with $d_{\mathrm{Ni}}=1.75$ Å, $d_{\mathrm{Ni\text{-}Cu}}=1.75$ Å and all Cu layers at the bulk spacing.

This is because the loss spectra depend on the coherent contributions from layers having large eigendisplacements. Since the film modes have displacements confined primarily in the Ni layers, their loss cross sections are particularly sensitive to the Ni spacings. We demonstrate this in Fig. 3, where the distance between Ni layers (d_{Ni}) is increased in steps of 0.1 Å. The best agreement is obtained for a Ni-Ni interlayer spacing of $d_{\mathrm{Ni}}=1.75$ Å. By varying the Ni spacing by merely 0.1 Å, i.e., at 1.85 Å or 1.65 Å, there is qualitative disagreement. From the calculated spectra of $d_{\mathrm{Ni}}=1.75$ Å, we see that the measured Ni-film loss peak is made up of two separate modes: X_1 and Z_2. Also, the data for the Rayleigh peak is due to S_4 and resonance modes in the Cu bulk band. The calculated film-mode loss peak is completely absent at 1.85 Å and shows up only as a small shoulder at 1.65 Å. We further determine the variation of the first Ni spacing. Using an R-factor analysis,[17] the best fit with data is obtained for $d_{\mathrm{Ni}}^{12}=1.7\pm0.1$ Å, and $d_{\mathrm{Ni}}^{23}=d_{\mathrm{Ni}}^{34}=d_{\mathrm{Ni\text{-}Cu}}=1.80\pm0.1$ Å. The Cu layers have the bulk spacing of 1.8 Å. These results are very similar to those found for 3-ML Ni/Cu(001) by a dynamical LEED study.[8]

The calculated dispersion curves using the surface lattice-dynamical model listed in Table I for the 2-ML Ni/Cu(001) system are shown in Fig. 4. The calculated dispersions again agree very well with the data for the 2-ML system (open circles). A structural analysis, using the R factor, yields a best agreement for $d_{\mathrm{Ni}}^{12}=1.75\pm0.1$ Å, $d_{\mathrm{Ni\text{-}Cu}}=1.75\pm0.1$ Å, and all the Cu layers at the bulk spacing. The loss spectra corresponding to the best structure is shown in Fig. 5. We see in Fig. 5(a) that along $\bar{\Gamma}\bar{X}$, the film mode Z_2 appears as a separate peak, above the peak of the Rayleigh mode. The situation is different along $\bar{\Gamma}\bar{M}$; an example is shown in Fig. 5(b), at $\zeta=0.84$ [$\zeta=q_{\parallel}/(1.74\ \text{Å}^{-1})$]. Here, the Rayleigh mode S_1 and a film mode (this film mode is dominated by the shear vertical motion of the second-layer Ni atoms) appear as a single peak in the data. In fact, from Fig. 5(b), we see that the measured peak is made up of the S_1 mode, a resonance mode, and this film mode. This accounts for the broad peak width in the data. Previous data[13] and the data presented here along $\bar{\Gamma}\bar{M}$ do not resolve the Ni-film modes as separate loss peaks. We see from the dispersion curves shown in Figs. 2 and 4 that this is due to the softening of force constants in the Ni film.

In summary, the phonon dispersions along the $\bar{\Gamma}\bar{X}$ and $\bar{\Gamma}\bar{M}$ directions of the Ni-film modes show considerable softening of the force constants in the Ni film. The electron-energy-loss cross sections are sensitive to interlayer spacings in the epitaxial film. With the surface Ni atoms at the Cu-Cu lateral spacings and the determined interlayer spacing of 1.75 Å, the area per unit cell is expanded by 5.3% while the interlayer spacing is contracted by 0.7%. This leads to an overall surface-volume expansion of 4.6% in the Ni film.

This work was supported by the U.S. Department of Energy under Grants No. DE-FG02-84ER45076 and No. DE-FG02-84ER45147, and by Petroleum Research Fund Grant No. 1154-AC5,6, administered by the American Chemical Society.

*Present address: Department of Chemistry, Arizona State University, Tempe, AZ 85187.

[1]For an excellent overview of metal-metal interfaces, see J. P. Biberian and G. A. Somorjai, J. Vac. Sci. Technol. **16**, 2073 (1979); E. Bauer, Appl. Surf. Sci. **11**, 479 (1982); E. Bauer and J. H. van der Merwe, Phys. Rev. B **33**, 3657 (1986).

[2]Z. Q. Wang, S. H. Lu, Y. S. Li, F. Jona, and P. M. Marcus, Phys. Rev. B **35**, 9322 (1987); Z. Q. Wang, Y. S. Li, F. Jona, and P. M. Marcus, Solid State Commun. **61**, 623 (1987).

[3]B. Heinrich, A. S. Arrott, J. F. Cochran, C. Liu, and K. Myrtle, J. Vac. Sci. Technol. **4**, 1376 (1986).

[4]S. A. Chambers, T. J. Wagener, and J. H. Weaver, Phys. Rev. B **36**, 8992 (1987); S. A. Chambers, S. B. Anderson, H.-W. Chen, and J. H. Weaver, *ibid.* **35**, 2592 (1987).

[5]W. F. Egelhoff, Jr., Phys. Rev. Lett. **59**, 559 (1987).

[6]C. L. Fu and A. J. Freeman, Phys. Rev. B **35**, 925 (1987).

[7]D. Pescia, G. Zampieri, M. Stampanoni, G. L. Bona, R. F. Willis, and F. Meier, Phys. Rev. Lett. **58**, 933 (1987); J. A. C. Bland, D. Pescia, and R. F. Willis, *ibid.* 58, 1244 (1987).

[8]M. A. Abu-Joudeh, B. M. Davies, and P. A. Montano, Surf. Sci. **171**, 331 (1986).

[9]A. Clarke, G. Jennings, R. F. Willis, P. J. Rous, and J. B. Pendry, Surf. Sci. **187**, 327 (1987).

[10]A. Clarke, P. J. Rous, M. Arnott, G. Jennings, and R. F. Willis, Surf. Sci. **192**, L843 (1987).

[11]L. L. Kesmodel, J. Vac. Sci. Technol. A **1**, 1456 (1983); L. L. Kesmodel, M. L. Xu, and S. Y. Tong, Phys. Rev. B **34**, 2010 (1986).

[12]Y. Chen, Z. Q. Wu, J. M. Yao, and S. Y. Tong, Phys. Rev. B **39**, 5617 (1989), and references therein.

[13]C. Stuhlmann and H. Ibach, Surf. Sci. **219**, 117 (1989).

[14]Mohamed H. Mohamed, Jae-Sung Kim, and L. L. Kesmodel, Phys. Rev. B **40**, 1305 (1989).

[15]Z. Q. Wu, Y. Chen, M. L. Xu, S. Y. Tong, S. Lehwald, M. Rocca, and H. Ibach, Phys. Rev. B **39**, 3116 (1989).

[16]Y. Chen, M. L. Xu, S. Y. Tong, M. Wuttig, W. Hoffmann, R. Franchy, and H. Ibach, Phys. Rev. B **42**, 5451 (1990).

[17]M. L. Xu and S. Y. Tong, Phys. Rev. B **31**, 6332 (1985).